Volume 13
Number 22
14 June 2022
Pages 6433–6754

Chemical Science

rsc.li/chemical-science

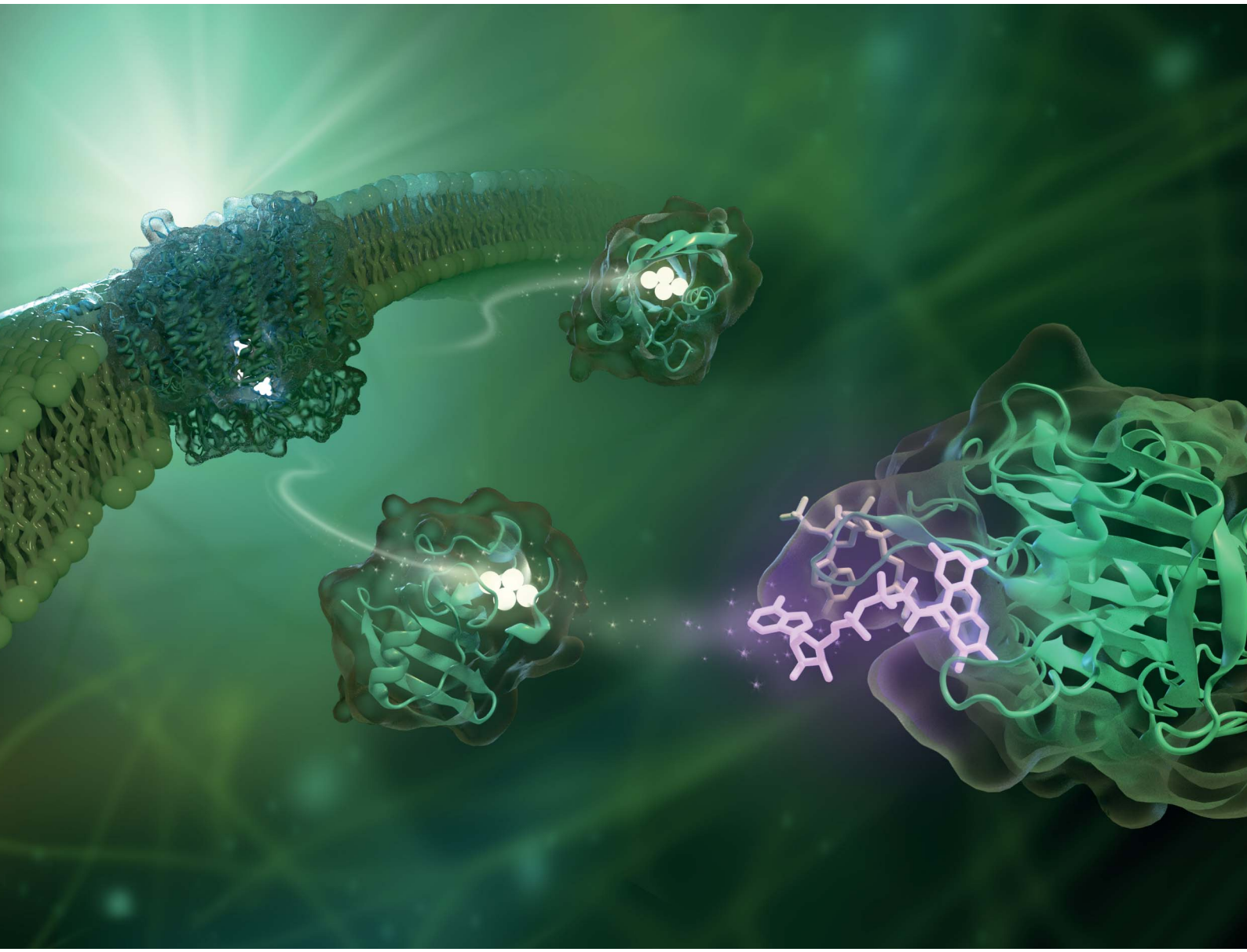

ISSN 2041-6539

ROYAL SOCIETY OF CHEMISTRY

EDGE ARTICLE

Lisa M. Utschig *et al.*

Biohybrid photosynthetic charge accumulation detected by flavin semiquinone formation in ferredoxin-NADP$^+$ reductase

Chemical Science

ROYAL SOCIETY OF CHEMISTRY

EDGE ARTICLE

View Article Online
View Journal | View Issue

Check for updates

Cite this: *Chem. Sci.*, 2022, **13**, 6502

All publication charges for this article have been paid for by the Royal Society of Chemistry

Open Access Article. Published on 11 May 2022. Downloaded on 2/9/2026 7:45:13 AM. This article is licensed under a Creative Commons Attribution-NonCommercial 3.0 Unported Licence.

Biohybrid photosynthetic charge accumulation detected by flavin semiquinone formation in ferredoxin-NADP$^+$ reductase†

Lisa M. Utschig,* Udita Brahmachari, Karen L. Mulfort, Jens Niklas and Oleg G. Poluektov

Flavin chemistry is ubiquitous in biological systems with flavoproteins engaged in important redox reactions. In photosynthesis, flavin cofactors are used as electron donors/acceptors to facilitate charge transfer and accumulation for ultimate use in carbon fixation. Following light-induced charge separation in the photosynthetic transmembrane reaction center photosystem I (PSI), an electron is transferred to one of two small soluble shuttle proteins, a ferredoxin (Fd) or a flavodoxin (Fld) (the latter in the condition of Fe-deficiency), followed by electron transfer to the ferredoxin-NADP$^+$ reductase (FNR) enzyme. FNR accepts two of these sequential one electron transfers, with its flavin adenine dinucleotide (FAD) cofactor becoming doubly reduced, forming a hydride which is then passed onto the substrate NADP$^+$ to form NADPH. The two one-electron potentials (oxidized/semiquinone and semiquinone/hydroquinone) are similar to each other with the FNR protein stabilizing the hydroquinone, making spectroscopic detection of the intermediate semiquinone state difficult. We employed a new biohybrid-based strategy that involved truncating the native three-protein electron transfer cascade PSI → Fd → FNR to a two-protein cascade by replacing PSI with a molecular Ru(II) photosensitizer (RuPS) which is covalently bound to Fd and Fld to form biohybrid complexes that successfully mimic PSI in light-driven NADPH formation. RuFd → FNR and RuFld → FNR electron transfer experiments revealed a notable distinction in photosynthetic charge accumulation that we attribute to the different protein cofactors [2Fe2S] and flavin. After freeze quenching the two-protein systems under illumination, an intermediate semiquinone state of FNR was readily observed with cw X-band EPR spectroscopy. The increased spectral resolution from selective deuteration allowed EPR detection of inter-flavoprotein electron transfer. This work establishes a biohybrid experimental approach for further studies of photosynthetic light-driven electron transfer chain that culminates at FNR and highlights nature's mechanisms that couple single electron transfer chemistry to charge accumulation, providing important insight for the development of photon-to-fuel schemes.

Received 16th March 2022
Accepted 2nd May 2022

DOI: 10.1039/d2sc01546c

rsc.li/chemical-science

Introduction

Fundamental mechanisms of photosynthetic solar energy conversion provide a road map for renewable and clean energy strategies. Nature's mechanisms incorporate both large transmembrane protein complexes and small soluble redox proteins in a Z-scheme electron transport chain of oxygenic photosynthesis for photon capture and conversion, utilizing the resultant chemical energy for water splitting and carbon dioxide assimilation. The primary solar energy conversion reactions occur in the transmembrane reaction center proteins (RCs) and involve rapid sequential electron transfers between a chain of protein embedded electron donor and acceptor molecules.[2] Following RC charge separation, the resultant electrochemical potential is converted to chemical energy by selective coupling to secondary reaction sequences. Electron paramagnetic resonance (EPR) spectroscopic studies have played a significant role in determining light-generated radical species and reactivities in RC electron transfer since they can selectively track the paramagnetic intermediates generated during the electron transfer events. Herein we build on these classic studies by using EPR methods to track and interrogate the photosynthetic electron transfer between the soluble redox proteins in the latter part of the Z-scheme (Fig. 1).

In oxygenic photosynthesis of higher plants, cyanobacteria, and algae, the photosystem II (PSII) and photosystem I (PSI) RCs operate in series to transfer electrons from water to NADP$^+$.[2] PSII conducts light-driven water oxidation,[3] whereas PSI

Chemical Sciences and Engineering Division, Argonne National Laboratory, Lemont, IL 60439, USA. E-mail: utschig@anl.gov

† Electronic supplementary information (ESI) available: Flavin oxidation and protonation states, additional EPR spectra, EPR simulation parameters, and NADP$^+$ reduction experiments. See https://doi.org/10.1039/d2sc01546c

© 2022 The Author(s). Published by the Royal Society of Chemistry

Open Access Article. Published on 11 May 2022. Downloaded on 2/9/2026 7:45:13 AM.
This article is licensed under a Creative Commons Attribution-NonCommercial 3.0 Unported Licence.

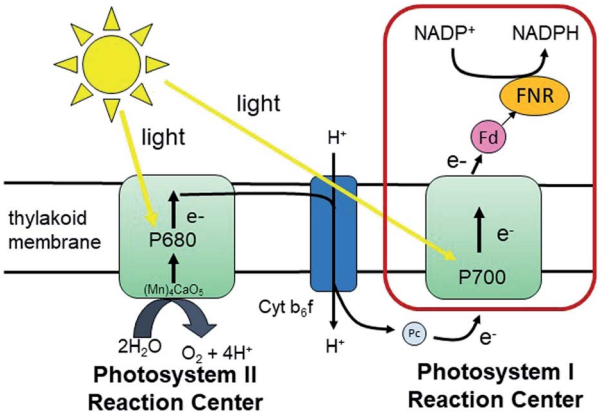

Fig. 1 The Z-scheme of electron transport in oxygenic photosynthesis. Photosystem II (PSII) absorbs photons that are used to oxidize water. The extracted electrons are passed on to photosystem I (PSI) *via* the cytochrome b_6f complex (Cyt b_6f) and the electron transfer protein plastocyanin (Pc). PSI carries out light-driven transmembrane electron transfer from Pc to ferredoxin (Fd) (or flavodoxin (Fld) under conditions of Fe-deficiency). Fd (or Fld) then shuttles the electrons from PSI to ferredoxin $NADP^+$-reductase (FNR) for the reduction of $NADP^+$ to NADPH that is used in carbon fixation. The red box highlights the electron transfer reactions of interest in this study.

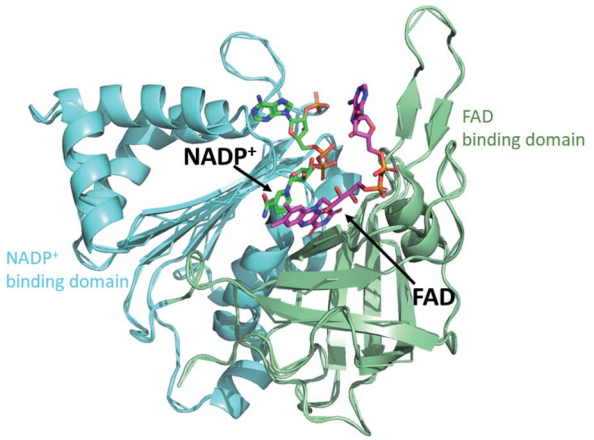

Fig. 2 Crystal structure of FNR. The protein folds into two domains, one domain (green) contains the FAD cofactor (purple) and the other domain (blue) contains $NADP^+$ (dark green). (2BSA) Fd/Fld dock at the interface of the two domains on the cofactor side (top of this view).

catalyzes light-driven transmembrane electron transfer from plastocyanin to oxidized ferredoxin (Fd) (eqn (1)).[4] The electrons from reduced Fd are used by the enzyme ferredoxin-$NADP^+$ reductase (FNR) for the reduction of $NADP^+$ to NADPH, the terminal step of the Z-scheme (eqn (2)). Under conditions of Fe-deficiency in cyanobacteria and some algae, flavodoxin (Fld) substitutes for Fd in the reduction of FNR.[5]

$$PSI + Fd^{3+} \xrightarrow{h\nu} PSI^+ + Fd^{2+} \quad (1)$$

$$2Fd^{2+} + NADP^+ + H^+ \xrightarrow{FNR} 2Fd^{3+} + NADPH \quad (2)$$

FNR contains a single flavin adenine dinucleotide (FAD) cofactor with an isoalloxazine ring which can stabilize three different oxidation states: fully oxidized, partially reduced by one electron (semiquinone), and fully reduced by two electrons (hydroquinone). FNR pairs single electrons from reduced Fd (or Fld) in a single hydride transfer step to protein bound substrate $NADP^+$.[6] Crystal structures of FNR reveal that the protein folds in two domains, one containing the noncovalently bound FAD molecule and the other $NADP^+$ (Fig. 2).[7,8] Fd and Fld can form 1 : 1 complexes with FNR. The active site for Fd/Fld docking is at the interface of the two domains.[9] Thus two reduced Fd or two reduced Fld proteins are needed for the formation of one NADPH molecule from a single FNR protein (eqn (2)). The two one-electron potentials of FAD are close to each other with FNR proteins stabilizing only 10–20% of the maximal amount of semiquinone.[10,11] Nevertheless, the FAD semiquinone state certainly plays a role in the enzyme-catalyzed reduction of $NADP^+$ as both Fd and Fld provide two successive one-electron reductions to FNR. To better understand photosynthetic coupling of one electron transfers to charge accumulation, we targeted generation of a stable semiquinone state of FNR for EPR characterization using the native electron transfer properties and interactions between the protein partners Fd and Fld.

Unlike Fld for which the semiquinone is exceptionally stable due to the relative midpoint potentials of the flavin mononucleotide (FMN) cofactor ($E_{OX/SQ}$ −195 mV; $E_{SQ/HQ}$ −390 mV), generation of a stable semiquinone species in FNR is challenging due to the similar midpoint potentials $E_{OX/SQ}$ −338 mV; $E_{SQ/HQ}$ −312 mV of the FAD cofactor and more positive potential of the hydroquinone.[11–13] Two methods have been used to generate the semiquinone of FNR for EPR studies, chemical reduction with NADPH or steady-state photoreduction using diazariboflavin in the presence of EDTA.[14–16] EPR/ENDOR spectroscopy has centered on a detailed examination of the localized molecular and electronic structural information of the flavin cofactor site in FNR.[15,17,18] In this work we have extended these studies with directed photoreduction of FNR *via* light-driven interprotein electron transfer. This method will allow us to generate the semiquinone signal in high yield, avoiding the difficulties associated with chemical reduction like double reduction or addition of other radical species in solution such as diazariboflavin. In addition, we will observe the semiquinone state for electron transfer competent Fd-FNR and Fld–FNR complexes. To accomplish the spectroscopic detection of the semiquinone state, we used a bioinorganic approach, replacing the light-initiated chemistry of PSI with biohybrid complexes comprised of a photosensitizer molecule, ruthenium(II) tris(bipyridine) (RuPS), covalently bound to Fd and Fld (RuFd and RuFld). The resultant biohybrids add light-driven electron transfer capability to their electron shuttle function in photosynthetic electron transfer. Recently photosynthetic-based biohybrids were built with non-native functionality for photocatalytic H_2 production.[19–24] Herein we have applied biohybrid-driven chemistry to look at native photosynthetic function to better understand nature's mechanisms.

To aid in probing the two-protein electron transfer cascades RuFd → FNR and RuFld → FNR, we employed a method

Open Access Article. Published on 11 May 2022. Downloaded on 2/9/2026 7:45:13 AM. This article is licensed under a Creative Commons Attribution-NonCommercial 3.0 Unported Licence.

pioneered over 60 years ago, the deuteration of photosynthetic microorganisms by adaption and growth of bacteria, cyanobacteria and algae in heavy water (99.7% D_2O).[25–27] EPR spectroscopy of deuterated photosynthetic proteins is a classic approach that helped determine the cofactors involved with the electron transfer events in RCs.[28–35] Deuteration often substantially increases EPR spectral resolution and provides the opportunity to directly probe flavin (in Fld) to flavin (in FNR) electron transfer *via* EPR for the first time. We targeted systematic study of Fd, a single electron carrier, Fld, a two electron carrier, and FNR, a two electron (hydride) transfer protein for insight on charge accumulation aspects of photosynthetic electron transfer in the latter part of nature's Z-scheme chemistry. The biohybrid methodologies developed inspire future study of ubiquitous flavin electron transfer chains in biology as well as inform artificial photosynthetic strategies for coupling single electron photochemistry to multielectron chemistry necessary for efficient photocatalytic solar fuel synthesis.

Results and discussion

Development of the two protein biohybrid system

Flavoproteins have the unique capacity of transferring either just one electron in each redox step or two electrons at once. Both FMN and FAD have an isoalloxazine ring, which is the redox active part of the flavin molecule (Fig. 3A). For this reason, nature incorporates flavoproteins in a wide variety of reaction schemes in addition to photosynthesis including energy transduction and biosynthesis.[36] As such, spectroscopic methods for probing involvement of flavin semiquinone intermediates in flavoenzyme-catalyzed reactions is of wide interest, but experimentally challenging. To investigate the flavin reactions in the latter part of the photosynthetic Z-scheme we first targeted modification of the native proteins in two ways: insertion of deuterated flavin cofactor and specific binding of RuPS.

Extracting significant quantities of deuterated FNR from cyanobacteria grown in 99.7% D_2O media would be difficult due to low yielding protein purification protocols. Therefore, we isolated deuterated Fld protein, from which we extracted and purified the deuterated FMN cofactor.[37] We confirmed successful deuterated flavin incorporation into FNR by UV-Vis spectroscopy (Fig. S1†). The ^{2}H-FMN cofactor inserted into unreconstituted FNR "FNR(^{2}H-FMN)" gave an acceptable $A_{280}/A_{456} = 7$, where for overexpressed FNR with <5% FAD cofactor after purification, $A_{280}/A_{456} = 54$. Crystal structures show that the FNR protein fold can productively use both FAD and FMN, as the adenosine moiety has no specific interactions with the protein.[7,38] To affirm this, we tested the functionality of FMN substitution for FAD in FNR. PSI-driven $NADP^+$ reduction activity is shown in Fig. S2.† Replacement of native FAD with ^{2}H-FMN in FNR does not produce significant differences in activity under the reaction conditions. A slight slowing of enzymatic activity 77 000 *vs.* 100 400 mol NADPH (mol PSI)$^{-1}$ h^{-1} and overall lower final quantity of NADPH formed was observed. This is most likely due to the FMN cofactor not positioning itself into the protein structure in exactly the same configuration as the native FAD cofactor, for which the protein was designed to hold. However, the same order of magnitude of activity indicates that selective deuteration of the flavin cofactor in FNR provides a highly functional system for EPR study.

RuPS (Fig. 3B) was covalently bound to free cysteine residues of Fd (Cys18) and Fld (Cys54) *via* a bromine substitution reaction to generate RuFd and RuFld.[20] The ICP-AES analysis showed near stoichiometric ratios of 1.0 ± 0.1 Ru/Fd and 1.2 ± 0.2 Ru/Fld. Covalent binding was confirmed with 5,5′-dithiobi(2-nitrobenzoic acid) modification of cysteine residues.[39] Upon illumination, RuFd and RuFld were able to drive $NADP^+$ reduction from FNR as shown in Fig. 4 using a 10-fold excess of RuFd or RuFld compared to FNR. Interestingly, RuFld-driven $NADP^+$ plateaued faster and achieved overall more turnovers per FNR than RuFd under the same experimental conditions. Initial rates were 8500 and 1050 mol NADPH (mol FNR)$^{-1}$ h^{-1} for RuFld and RuFd respectively (Fig. S3†). This difference is interesting and may be related to the difference in 1 electron *vs.* 2 electron carrying abilities of Fd *versus* Fld, as discussed below. Note, employing the simplified 2-protein system averts a potential pitfall in EPR studies of using the native electron transfer cascades PSI → Fd → FNR and PSI → Fld → FNR to observe FNR semiquinone intermediates. In the native 3-protein system the prominent light-generated $P700^+$ signal at $g = 2.00$ would significantly overlap with the semiquinone signal of FNR, making resolution of the semiquinone

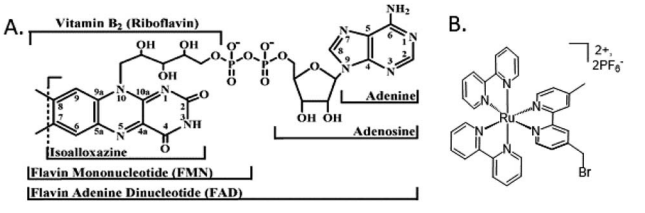

Fig. 3 Molecular cofactors used in this study. (A) Chemical structures of flavin adenine dinucleotide, FAD, the native cofactor of ferredoxin-$NADP^+$ reductase (FNR) and flavin mononucleotide, FMN, the native cofactor of flavodoxin (Fld).[1] (B) The ruthenium photosensitizer (RuPS), $[Ru(4\text{-}CH_2Br\text{-}4'\text{-}CH_3\text{-}2,2'\text{-bpy})(bpy)_2]\cdot 2PF_6$.

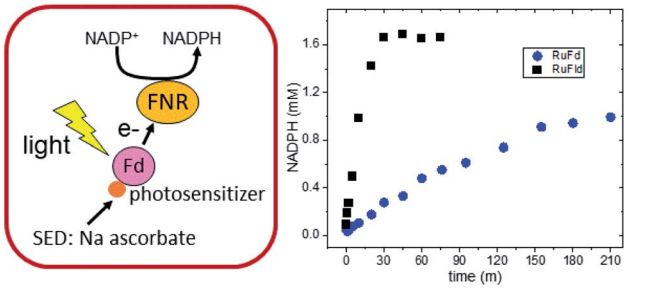

Fig. 4 Biohybrid photosynthetic $NADP^+$ reduction. (left) Schematic of the light-driven two protein cascade that replaces PSI with a ruthenium photosensitizer molecule bound to Fd. Fld can be substituted for Fd. (right) *In vitro* light-driven $NADP^+$ reduction *via* RuFd (blue circles) and RuFld (black squares).

© 2022 The Author(s). Published by the Royal Society of Chemistry

Open Access Article. Published on 11 May 2022. Downloaded on 2/9/2026 7:45:13 AM.
This article is licensed under a Creative Commons Attribution-NonCommercial 3.0 Unported Licence.

signal difficult. As the $NADP^+$ reduction assays show, RuFd and RuFld are able to carry out light-driven NADPH formation and are thus suitable biohybrids to replace PSI chemistry in EPR studies of semiquinone formation in FNR.

EPR studies: electron transfer from ferredoxin to FNR

The light-driven chemistry of our two protein cascade biohybrid systems was examined with cw X-band EPR spectroscopy. The single flavin cofactor of FNR proceeds through three oxidation states in the transfer of electrons from Fd to $NADP^+$, oxidized (FNR_{OX}), semiquinone (FNR_{SQ}) and hydroquinone (FNR_{HQ}) (Fig. S5†).[5] Of these three, only the FNR_{SQ} state has an unpaired electron that can be observed with EPR spectroscopy. We employed selective deuteration to aid in our detection of FNR_{SQ}.

We first examine the electron transfer RuFd → FNR. Fig. 5A shows the EPR spectra observed for FNR substituted with ^{1}H-FAD, ^{1}H-FMN, and ^{2}H-FMN. The paramagnetic semiquinone state was generated by illumination with freeze trapping techniques of a sample containing both RuFd and FNR proteins in solution at a ratio of 2 : 1 with the sacrificial electron donor (SED) sodium ascorbate. In each case, a typical flavin semiquinone signal centered at $g = 2.004$ is observed. The spectrum of $FNR(^2H\text{-}FMN)_{SQ}$ is different than the signals of the two FNR samples with protonated cofactors, $FNR(^1H\text{-}FMN)_{SQ}$ and $FNR(^1H\text{-}FAD)_{SQ}$. Deuteration of FMN effectively decreases the inhomogeneous line width of the EPR signal that is largely due to unresolved proton (also called ^{1}H in the following) hyperfine interactions. The substitution of ^{1}H by ^{2}H at nonexchangeable hydrogen positions on the flavin molecule results in a decrease in the hydrogen hyperfine coupling constants (relative gyromagnetic ratio of $^1H/^2H \approx 6.5$) so that the large hyperfine coupling constants of nitrogens and exchangeable hydrogen can be observed (protonated buffer).[37] Thus, substitution of the native ^{1}H-FAD cofactor with a non-native ^{2}H-FMN cofactor gives a distinctive EPR signal that can be readily studied. Comparison of the EPR signal observed in H_2O to that in D_2O (Fig. S6†) shows a line narrowing, consistent with a neutral semiquinone species *vs.* anionic species as the exchangeable proton has stronger hyperfine coupling compared to deuteron (Table S1 and Fig. S5†). Freeze trapping of samples illuminated at room temperature was necessary to generate a large semiquinone signal as only very small signals are observed for samples that were dark adapted prior to freezing in liquid nitrogen and illuminated at 20 K in the EPR cavity. Based on the intensity of the FNR_{SQ} signal formed after freeze trapping upon room temperature illumination, less than 5% low temperature electron transfer occurs between RuFd and FNR for samples frozen in the dark and illuminated at 20 K.

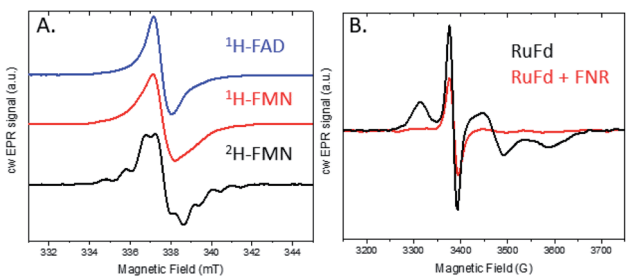

Fig. 5 cw X-band EPR spectra of the two protein systems RuFd and FNR (both ^{1}H). (A) Semiquinone signal for FNR reconstituted with ^{1}H-FAD (blue), ^{1}H-FMN (red), and ^{2}H-FMN (black), all three samples containing RuFd : FNR in a 2 : 1 ratio. (B) Light-induced reduction of the [2Fe2S] cluster of RuFd in the presence (red) and absence of FNR (black). Samples were illuminated at room temperature for 5 s followed by immersion in liquid N_2 while continuously illuminating. The ^{1}H-FMN sample contained 486 μM RuFd, 270 μM FNR. The ^{1}H-FAD sample contained 620 μM RuFd and 330 μM FNR. The ^{2}H-FMN sample contained 620 μM RuFd and 287 μM FNR.

EPR can also shed light on the biohybrid-driven interprotein electron transfer event that proceeds FNR_{SQ} formation. In the RuFd hybrid, RuPS can transfer electrons to the [2Fe2S] cluster of Fd *via* either an oxidative or reductive quenching mechanism in the presence of sodium ascorbate. Upon illumination of the RuFd hybrid in the presence or absence of FNR with freeze trapping techniques, we do not observe formation of a Ru(III) species which would be indicative of an oxidative quenching mechanism for RuPS*.[22] A reductive quenching pathway is probable due to the presence of a high concentration of the SED ascorbate.[40] However we were unable to detect a ligand centered reduction of RuPS for a $[Ru(bpy)_3]^+$ species by EPR so the mechanism remains uncertain.

In the native three-protein electron transfer cascade PSI → Fd → FNR, the [2Fe2S] cofactor of Fd (E_m −420 mV *vs.* NHE) shuttles a single electron from PSI to FNR. Does the RuFd → FNR electron transfer proceed through the [2Fe2S] cluster as well? Illumination of RuFd in the presence of sodium ascorbate with freeze trapping techniques leads to the formation of an EPR signal consistent with reduced [2Fe2S] cluster, $g_x = 2.05$, $g_y = 1.96$, $g_z = 1.89$ (Fig. 5B).[22,41] Thus, RuFd is capable of photoinduced electron transfer from the covalently bound RuPS to the [2Fe2S] cluster. In the presence of FNR, however, the signal corresponding to reduced [2Fe2S] is absent upon freeze trapping under illumination. This suggests that none of the light-generated electrons reside on the [2Fe2S] cluster; all electrons are transferred to FNR. However, whether or not electron transfer from RuPS to FNR in the RuFd-FNR complex proceeds through the [2Fe2S] cluster cannot be determined from EPR alone. For this reason, we prepared the Ru-apoFd analogue in which the [2Fe2S] cluster has been removed.[42] $NADP^+$ reduction experiments using photoexcitation of Ru-apoFd show a slightly faster rate of NADPH formation (1400 mol NADPH (mol FNR)$^{-1}$ h^{-1}) *vs.* the biohybrid prepared with native Fd (1050 mol NADPH (mol FNR)$^{-1}$ h^{-1}) (Fig. 6A). Based on these results, the [2Fe2S] cluster is not essential for NADPH formation. RuPS is a one electron donor. Therefore, in the case of apo-Fd, one electron is transferred directly from RuPS to FAD of FNR.[43] This direct electron transfer must occur two times, to produce a hydride that yields NADPH. For native Fd, the electron transfer occurs step-wise: first from RuPS to [2Fe2S], then from [2Fe2S] to FAD of FNR. This step-wise electron transfer occurs two times to produce the hydride that yields NADPH (Fig. 7). A hypothesis that is consistent with redox potentials and EPR and explains the difference in NADPH production between RuFd

Open Access Article. Published on 11 May 2022. Downloaded on 2/9/2026 7:45:13 AM.
This article is licensed under a Creative Commons Attribution-NonCommercial 3.0 Unported Licence.

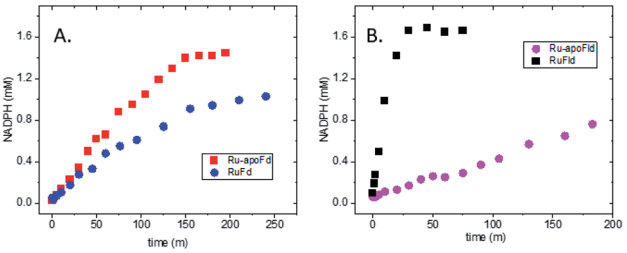

Fig. 6 Importance of the intermediate electron acceptor cofactors in biohybrid photosynthetic $NADP^+$ reduction. (A) *In vitro* light-driven $NADP^+$ reduction for RuFd (blue circle) and Ru-apoFd (red square). (B) *In vitro* light-driven $NADP^+$ reduction for RuFld (black square) and Ru-apoFld (magenta circle).

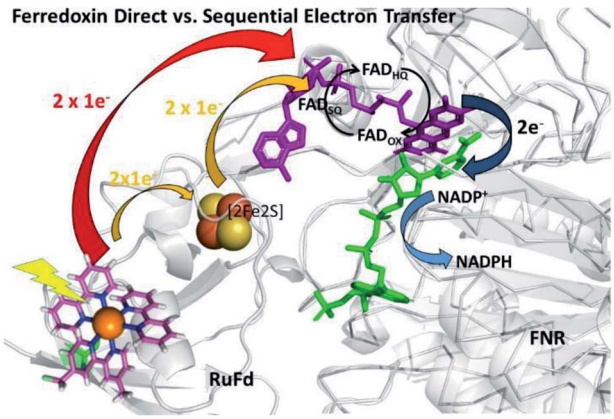

Fig. 7 Scheme of photosynthetic electron transfer between RuFd and FNR showing two potential interprotein electron transfer pathways: a direct route between RuPS and FNR (red arrow) or a sequential transfer through the [2Fe2S] cluster of Fd to FNR. (Orange arrows). The [2Fe2S] cluster can accept one electron at a time, and donate one at a time. After receiving 2 single electron transfers from photoexcited RuFd, FNR_{HQ} then donates 2 electrons in one step *via* a hydride to the bound substrate $NADP^+$ to form NADPH. Reduced Fd and FNR_{SQ} are observable *via* EPR. (PDB ID: 1A70, 2BSA).

and Ru-apoFd (Fig. 6A) is that one ET step is faster than two steps depending on the relative orientations of the two proteins as they dock together.

EPR studies: electron transfer from flavodoxin to FNR

We next examined the RuFld → FNR reaction, which provides a unique, yet challenging, opportunity to examine flavoprotein to flavoprotein electron transfer with EPR spectroscopy. Fld contains a FMN cofactor for shuttling a single electron from PSI to FNR. Like Fd, Fld forms a 1 : 1 complex with FNR. The FMN semiquinone in Fld is highly stable, so that close to 100% of the flavin is in this form after addition of one electron.[44] This is a consequence of the relative midpoint potential for the Fld_{OX}/Fld_{SQ} couple (−195 mV) and the Fld_{SQ}/Fld_{HQ} couple (−390 mV).[13] Note, the Fld_{SQ}/Fld_{HQ} pair is believed to shuttle electrons between PSI and FNR for the formation of NADPH.[6] The study of the electron transfer between Fld and FNR by means of optical transient absorption spectroscopy is difficult because it is hard to detect the one electron transfer: one semiquinone flavin species gets oxidized (FMN in Fld) and a new semiquinone flavin species gets generated (FAD in FNR); both flavins exhibit optical spectral similarities if they are in the same redox state.[13] Likewise, previous EPR studies of the Fld–FNR complex for fully protonated systems achieved formation of a semiquinone signal, but the EPR signals could not be distinguished between Fld_{SQ} and FNR_{SQ}.[15]

We investigated this process using a selective deuteration approach. RuFld biohybrids were made using both fully deuterated Fld and protonated Fld (both in protonated buffer). Freeze quenching of these illuminated biohybrids in the presence of SED ascorbate resulted in a signal of the Fld semiquinone with g-value of 2.004 (Fig. 8A). The hyperfine splitting pattern of ^{2}H-Fld is similar to ^{2}H-FMN in FNR (black spectrum in Fig. 5A), indicating that the same paramagnetic flavin species is trapped. A good spectral simulation (Fig. 8A, green) was obtained assuming one strongly coupled proton in addition to the two prominent nitrogen atoms in the isoalloxazine moiety (see Table S1† for simulation parameters). Since the flavin is fully deuterated, this must be due to an exchangeable proton. Indeed, very good agreement is found with published values[45] for neutral flavin semiquinones protonated at position 5 (Fig. 3A, Table S2†). Importantly, the ^{2}H-Fld and ^{1}H-Fld have identifying spectral features which can be used to examine inter flavoprotein electron transfer.

Matched samples were prepared, ^{2}H-Fld + FNR(^{1}H-FMN) and ^{1}H-Fld + FNR(^{2}H-FMN), with the goal of using the differences in isotopes between the flavin cofactors to track the RuFld → FNR electron transfer event. Interflavin electron transfer is spectroscopically complicated due to the multiple redox and protonation states of flavins,[13] and only the semiquinone state is observed by EPR (Fig. S5†). Note, Fld_{HQ} delivers one electron at a time to FNR_{OX}, forming first the intermediate FNR_{SQ}, then FNR_{HQ}. After electron transfer, Fld_{SQ} is formed.

Fig. 8B shows the cw X-band EPR spectra of the selectively deuterated samples, Ru(^{2}H-Fld) + FNR(^{1}H-FMN) and Ru(^{1}H-Fld) + FNR(^{2}H-FMN), measured after freeze trapping under illumination to generate semiquinone signals. The samples contained

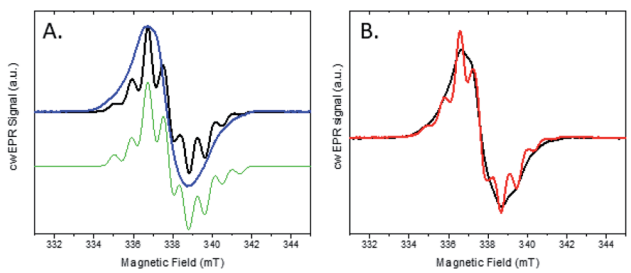

Fig. 8 cw X-band EPR spectra of the two protein systems RuFld and FNR. (A) Semiquinone signal for the RuFld hybrid for ^{1}H-Fld (blue) and ^{2}H-Fld (black). Samples contained 260 μM Ru(^{1}H-Fld) and 360 μM Ru(^{2}H-Fld). Simulated spectrum of ^{2}H-Fld (green), parameters Table S1.† (B) Mixed isotope strategy for defining flavin to flavin electron transfer, Ru(^{1}H-Fld) + FNR(^{2}H-FMN) (black) and Ru(^{2}H-Fld) + FNR(^{1}H-FMN) (red). Protein concentrations were: 400 μM Ru(^{1}H-Fld), 280 μM FNR(^{2}H-FMN), 230 μM Ru(^{2}H-Fld), 200 μM FNR(^{1}H-FMN).

© 2022 The Author(s). Published by the Royal Society of Chemistry

Open Access Article. Published on 11 May 2022. Downloaded on 2/9/2026 7:45:13 AM.
This article is licensed under a Creative Commons Attribution-NonCommercial 3.0 Unported Licence.

both RuFld and FNR proteins in solution at a ratio of 1.4 : 1 as well as SED ascorbate. Comparison with ^{1}H-Fld and ^{2}H-Fld spectra in Fig. 8A unambiguously shows that both spectra in Fig. 8B are dominated by the signal of Fld_{SQ}. However, spectral differences due to the presence of a smaller contribution of FNR_{SQ} are observed. To determine the relative contribution from these two radicals both spectra were simulated as a sum of Fld_{SQ} and FNR_{SQ} spectra with different weight factors, normalized for the second integral. Using this conventional deconvolution procedure, we determine that 13% of the total EPR signal is due to FNR_{SQ} generated *via* interprotein electron transfer. As observed in the $NADP^+$ reduction assay, RuFld is capable of driving photocatalytic NADPH formation from FNR (Fig. 6B). The EPR spectral results are consistent with efficient light-driven electron transfer between RuFld and FNR. A hypothesis supported by the EPR results is that the flavin cofactor of Fld is reduced first by a reductive quenching mechanism of RuPS* by ascorbate, followed by rapid one electron transfers to the flavin cofactor of FNR, producing its semiquinone form (FNR_{SQ}) which is in equilibrium with the EPR silent hydroquinone state, FNR_{HQ}. The 13% FNR_{SQ} observed by our selective deuteration scheme is in accord with the reported 10–20% FNR protein stabilization of the maximal amount of semiquinone and consistent with flavoproteins that transfer 2 electrons at a time.[9,10]

To further examine flavin cofactor involvement in RuFld → FNR interprotein electron transfer, we removed the FMN cofactor from Fld and prepared the Ru-apoFld biohybrid. The capability of Ru-apoFld to transfer light-generated electrons to FNR was measured in the $NADP^+$ reduction assay (Fig. S4†) As Fig. 6B shows, removal of the flavin cofactor from Fld severely reduced the capability of the Ru-apoFld hybrid to efficiently drive $NADP^+$ reduction upon illumination. The 630 mol NADPH (mol FNR^{-1}) h^{-1} rate is 13-fold slower than that observed for the biohybrid made with native Fld, which confirms that the FMN cofactor in Fld is involved in the light-driven biohybrid RuFld → FNR electron transfer process. We assert that the multielectron capability of the flavin cofactor facilitates the two electron $NADP^+$ reaction; providing an excellent example of photosynthetic charge accumulation. Fig. 9 depicts the scheme for light driven RuFld → FNR electron transfer NADPH formation. RuPS is a one electron donor, so to initiate the process RuPS must donate one electron two times to the FMN cofactor of Fld to generate Fld_{HQ}. Fld_{HQ} donates an electron to FAD cofactor of FNR. The Fld protein then cycles between the Fld_{SQ} and Fld_{HQ} states as it accepts one electron from RuPS and donates one electron to FAD cofactor of FNR. After FAD cofactor of FNR receives two electrons, it produces the hydride that yields NADPH.

Nature's mechanisms for coupling single electron transfers to charge accumulation

Nature has optimized the photosynthetic molecular machinery that couples single electron transfers, generated at the PSI RC protein, to charge accumulation at the FNR protein. Fd and Fld proteins shuttle light-generated electrons between PSI and FNR.

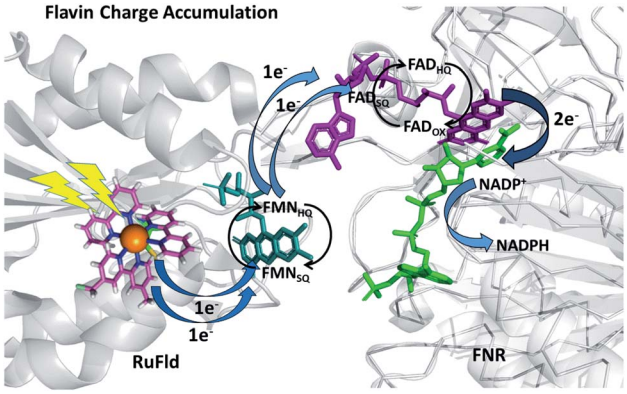

Fig. 9 Scheme of photosynthetic electron transfer between RuFld and FNR highlighting the multielectron capabilities of the flavin cofactors. To initiate the interprotein electron transfer, Fld_{ox} must obtain two electrons from single electron transfers from RuPS covalently bound to Cys54 (RuPS is rereduced *via* the sacrificial electron donor sodium ascorbate). The Fld cofactor then cycles between the Fld_{SQ} and Fld_{HQ} transferring electrons one at a time to FNR. FNR_{HQ} then donates 2 electrons in one step *via* a hydride to bound $NADP^+$ to form NADPH. Fld_{SQ} and FNR_{SQ} are observable *via* EPR. (PDB ID: 1CZN, 2BSA).

Both are similarly capable of doing so, as demonstrated in PSI-driven *in vitro* $NADP^+$ reduction experiments, with observed rates of 92 500 mol NADPH (mol FNR^{-1}) h^{-1} and 100 400 mol NADPH (mol FNR^{-1}) h^{-1} for Fld and Fd respectively (Fig. S7†). A surprising difference was revealed when we examined our biohybrid systems in which PSI was replaced with a molecular RuPS covalently bound to Fd and Fld. The RuFld biohybrid system exhibited an 8-fold higher rate of $NADP^+$ reduction and nearly double the number of turnovers than our RuFd system (Fig. 4). The E_m values for Fd (−420 mV *vs.* NHE) and Fld (−390 mV *vs.* NHE) are similar, ruling out driving force as the cause of the reactivity differences.

What is the molecular basis for this difference? With interprotein electron transfer, multiple factors are at play which make it experimentally difficult to address this question, but we can propose several likely rationale. One possibility is that the RuPS molecule bound to the protein surface interferes with protein–protein interactions. This could alter distances between the protein cofactors involved in electron transfer (most likely increasing them), thus impacting electron transfer rates. Fd (10.5 kDa) is smaller than Fld (17 kDa) so RuPS is a larger relative surface area of Fd than Fld, and more likely to disrupt structure and be a steric hindrance for RuFd- FNR complexation compared to RuFld–FNR complexation. A prior study, however, showed that covalent linkage of RuPS to the Fd protein did not limit formation of a competent RuFd–FNR complex for interprotein electron transfer and reported a rate of 6500 s^{-1} for the RuFd to FNR light-driven electron transfer reaction.[43] Multiple orientations are available for Fd docking if in fact RuPS interferes with a particular interaction as a range of binding interactions for Fd have been observed in Fd-FNR crystal and NMR structures, with inter flavin isoalloxazine and [2Fe2S] distances < 8 Å.[46–49] Crystal structures of Fld–FNR

Open Access Article. Published on 11 May 2022. Downloaded on 2/9/2026 7:45:13 AM. This article is licensed under a Creative Commons Attribution-NonCommercial 3.0 Unported Licence.

remain elusive, and it has been postulated that the interaction of Fld with FNR is less specific that of Fd.[5] Perhaps this added flexibility in binding orientations aids in productive RuFld-FNR formation, facilitating the interprotein electron transfer. Quantum yields of electron transfer and intra and interprotein electron transfer rates may affect the overall reaction rates for $NADP^+$ reduction.

Another possibility is that the RuPS molecule itself is not the sole cause of altered interprotein electron transfer, but rather brings to light, by way of the biohybrid system, a feature of nature's photosynthetic mechanism not observed before. Since a notable difference between Fd and Fld is the distinct type of cofactors, a [2Fe2S] cluster and a flavin molecule, we hypothesize that the higher rate of $NADP^+$ reduction observed for RuFld → FNR *versus* RuFd → FNR light-driven electron transfer is due to the nature of the flavin cofactor; that is its ability to cycle between redox states of the semiquinone and hydroquinone (Fig. 9) compared to the less versatile single electron shuttling character of an Fe–S cluster (Fig. 7). We believe the difference between Fd and Fld is not observed in the PSI-driven system due to evolutionary optimization. Even *in vitro*, the observed rates of $NADP^+$ reduction are 2 orders of magnitude faster than the rates we observe for our Ru biohybrid driven systems. Any differences due to the nature of the cofactors of Fd and Fld are obscured by the overall efficiency of the PSI-driven system. Thus, by using the biohybrid system we have uncovered an interesting observation about photosynthetic coupling of one electron transfers to charge accumulation.

Further investigation of flavin-based biohybrids can inform purely artificial systems about mechanisms and design strategies for light-induced charge accumulation. Artificial photosynthetic systems have been constructed that mimic structural and functional components of nature's light driven chemistry, yet it remains difficult to accomplish charge accumulation in purely synthetic systems.[50,51] Photosynthetic biohybrid and artificial systems that accomplish charge accumulation are of interest in solar fuel schemes where efficient delivery of multiple electrons is needed. Understanding general mechanisms of charge accumulation is thus important for development of strategies for solar fuel development. Biohybrids experimentally bridge the gap between artificial and natural systems, combining beneficial features of both systems, which can provide new chemical insight.[52]

Conclusions

PSI-driven electron transfer events result in the charge accumulation of two successive electrons at the FAD cofactor site of FNR protein. A combined biohybrid and selective deuteration approach was used to generate and spectroscopically detect with EPR the semiquinone state of FNR formed following light-driven single interprotein electron transfer from the electron shuttle proteins Fd and Fld. In $NADP^+$ reduction assays, a notable difference in RuFd *versus* RuFld reactivity was observed. The biohybrid technique revealed differentiated chemistry between the electron shuttle proteins, providing an example of the utility of incorporating synthetic molecules to creatively probe nature's mechanisms. We hypothesize that the observed differences are related to the versatility of flavin cofactors having three oxidation states readily available, and theorize that this intrinsic characteristic aids in photosynthetic charge accumulation at the FAD cofactor site of FNR. As such, this system provides a reminder of the evolutionary advantage of the functional inclusion of flavins in biological reaction schemes. Even though nature has mastered charge accumulation *via* photosynthetic schemes, it is still complicated to experimentally identify the individual mechanistic steps because of the multiple redox states of flavoproteins. Selective deuteration will enable application of advanced EPR techniques, such as high-field Mims-type pulsed electron-nuclear double resonance spectroscopy (ENDOR) or "matrix" ENDOR,[53–56] to interrogate the local flavin site protein environmental responses to electron transfer events in future experiments. We expect using biohybrids to explore integral functional components of solar energy conversion will provide important insight about fundamental mechanisms of photochemical energy conversion.

Experimental

Preparation of Fd and Fld biohybrids

The ruthenium photosensitizer (RuPS), $[Ru(4\text{-}CH_2Br\text{-}4'\text{-}CH_3\text{-}2,2'\text{-}bpy)(bpy)_2]\cdot 2PF_6$, was synthesized and characterized according to published methods.[57,58] The RuFd hybrid was prepared using *Spinacia oleracea* ferredoxin (Fd) from Sigma-Aldrich.[22] Spinach Fd (1.2 mM stock in 20 mM Hepes pH 7.9) was diluted to 32 μM in 10 mM MES buffer pH 6.0 and incubated with 8 mol equiv. RuPS (9.0 mM stock solution in DMSO) overnight at 4 °C. Samples were concentrated with Amicon 3000 MWCO filtration devices and repeatedly diluted (4 times) with 10 mM MES pH 6.0 to remove the unbound RuPS.

Ru-^{2}H-Fld hybrid was prepared using deuterated Fld isolated from *Thermosynechococcus lividus* (PCC6717) grown in deuterated medium and purified with protonated buffers.[59] Ru-^{1}H-Fld hybrid was prepared using Fld overexpressed in *E. coli* by standard procedures. UV-Vis spectroscopy of the purified ^{1}H-Fld showed low incorporation of the native FMN cofactor. Fld was reconstituted by addition of 4 mol equiv. FMN followed by removal of excess unbound FMN by extensive washing with 3000 MWCO filtration devices until the filtrate was colorless. RuPS binding to ^{2}H-Fld and ^{1}H-Fld was performed by adding 4 mol equiv. RuPS/Fld (150 μM Fld) in 20 mM Hepes pH 8.0. The sample was tumbled (LabQuake) overnight at 4 °C in the dark. Unbound RuPS was removed by microfiltration (Amicon 3000 MWCO) using 20 mM Hepes pH 8.0.

Apo-Fd and Apo-Fld were prepared by cofactor removal as reported previously by a trichloroacetic acid precipitation in the presence of dithiothreitol.[2,20,42] RuPS was bound to the apoproteins using the same methods as for the native holoproteins.

Inductively coupled plasma atomic emission spectroscopic (ICP-AES) measurements with a Thermo Scientific iCAP6000 spectrometer were used to calculate metal-to-protein ratios using comparison to known metal standards. Fd protein concentration was determined using UV-visible absorption and

© 2022 The Author(s). Published by the Royal Society of Chemistry

Open Access Article. Published on 11 May 2022. Downloaded on 2/9/2026 7:45:13 AM. This article is licensed under a Creative Commons Attribution-NonCommercial 3.0 Unported Licence.

a molar extinction coefficient of 9600 M^{-1} cm^{-1} at 422 nm or direct Fe content by ICP-AES.[60] Fld protein content was determined by the Bradford protein assay method.[61] Holo-Fld content was also verified with an extinction coefficient of 8300 M^{-1} cm^{-1} at 465 nm.[59] RuPS driven $NADP^+$ reduction activity was measured to verify successful interprotein electron transfer between the biohybrids and FNR protein. 4.8 μM biohybrid (RuFd, Ru-apoFd, RuFld, Ru-apoFld) was mixed with 500 nM FNR in a 20 mM Hepes pH 8.0 buffer containing 100 mM sodium ascorbate and 2 mM $NADP^+$ (Sigma Aldrich) as substrate. Photoreduction was assayed by sample illumination with 455 nm LED (Thorlabs) in 2 mm cuvette and UV-Vis spectra obtained at time points after illumination (Fig. S3 and S4†). NADPH formed was determined using the extinction coefficient 6.22 mM^{-1} cm^{-1} at 340 nm.[62]

Preparation of protonated FNR

FNR was overexpressed from a synthetic gene encoding a domain from *Anabaena* PCC7119 (Uniprot P21890, amino acids 137-440) and purified as previously detailed.[42] UV-Vis spectroscopy of the purified FNR protein showed low incorporation of the native FAD cofactor. To prepare protonated FNR EPR samples, the native FAD was reconstituted into purified FNR protein as verified by UV-Vis spectroscopy. FNR concentration was determined by extinction coefficient at 456 nm of 10 740 M^{-1} cm^{-1} and verified separately by Bradford protein assays.[42]

Preparation of FNR (^{2}H-FMN)

^{2}H-FMN cofactor was extracted from deuterated Fld by trichloroacetic acid precipitation in the presence of dithiothreitol. The solution was neutralized with addition of NaOH to pH 8.0 and rotovapped to 1 ml. The sample was passed through a Sephadex G25 column equilibrated with MilliQ water, heart cut fractions combined, rotovapped to dryness, and stored at −20 °C. Stock solution of ^{2}H-FMN was prepared by dilution with 20 mM Hepes pH 8.0 (in H_2O) and concentration determined with extinction coefficient at 450 nm 12 500 M^{-1} cm^{-1}. ApoFNR (overexpressed FNR with <10% FAD cofactor) was reconstituted with ^{2}H-FMN by addition of 5.8 mol equiv. FMN/FNR and overnight incubation. Unbound FMN cofactor was removed by microfiltration and washing with 20 mM Hepes pH 8.0 (protonated buffer). ^{2}H-FMN incorporation into FNR was verified by UV-Vis spectroscopy. To verify function of FMN substituted FNR, $NADP^+$ reduction was measured *via* PSI light-driven chemistry. Protein concentrations in the assay were 60 nM PSI purified from *Synechococcus leopoliensis* (UTEX625), 500 nM FNR, 4 μM Fd, and 10 μM cyt c_6 purified from *Thermosynechococcus lividus*. The reaction mixture contained 20 mM Hepes pH 8.0, 10 mM sodium ascorbate, 3 mM $MgCl_2$, 60 μM DCPIP, 0.03% *n*-dodecyl-β-maltopyranoside with 2 mM $NADP^+$ substrate (Sigma Aldrich). UV Vis spectra were taken prior to and at specific time points of sample illumination with a white light LED (Solis-3C, Thorlabs).

EPR experiments

Ru biohybrids and FNR samples were prepared as described above and concentrated to 300–600 μM in 20 mM Hepes pH 7.97 (all EPR samples in protonated buffer, except for sample specifically exchanged into deuterated buffer, spectrum shown in Fig. S6†). For interprotein electron transfer experiments, the RuFd or RuFld was combined in appropriate ratio with FNR(^{1}H-FAD), FNR(^{1}H-FMN) or FNR(^{2}H-FMN) in 100 mM sodium ascorbate and 120 mM NaCl. Samples were placed in quartz EPR tubes in a nitrogen box. A Bruker ELEXSYS II E500 EPR spectrometer (Bruker Biospin, Rheinstetten, Germany) equipped with a TE_{102} rectangular resonator (Bruker ER4102ST) and a helium gas-flow cryostat (ICE Oxford, UK) was used for cw X-band EPR measurements. An ITC (Oxford Instruments, UK) was used for temperature control. Dark spectra were obtained for all samples prior to illumination experiments. Samples were dark adapted in a nitrogen box prior to freezing in liquid nitrogen. Illumination during EPR measurements were performed using a white light LED (Solis-3C, Thorlabs). Samples were illuminated at room temperature for 5 s, followed by immersion in liquid N_2 while continuously illuminating, and then placed in a precooled EPR resonator. All EPR spectra were obtained at 20 K. Data processing was performed using Xepr (Bruker Biospin, Rheinstetten, Germany) and spectral simulation using the EasySpin program[63] in Matlab™ R2018b (MathWorks, Natick) environment.

Conflicts of interest

There are no conflicts to declare.

Data availability

Data are available upon request from the authors.

Author contributions

L. M. U. conceived the project. U. B. prepared proteins. L. M. U. prepared the biohybrid complexes and conducted the biohybrid experiments. K. L. M. performed molecular synthesis. J. N. and O. G. P. performed the EPR spectroscopy and spectral data analysis. L. U. wrote the manuscript. All authors discussed the results and contributed to manuscript editing.

Acknowledgements

The authors thank A. Wagner for growth of the cyanobacteria and P. Pokkuluri for overexpression of Fld and FNR. This work is supported by the U. S. Department of Energy, Office of Science, Office of Basic Energy Sciences, Division of Chemical Sciences, Geosciences, and Biosciences, under Contract No. DE-AC02-06CH11357.

Notes and references

1 Y.-T. Kao, C. Saxena, T.-F. He, L. Guo, L. Wang, A. Sancar and D. Zhong, *J. Am. Chem. Soc.*, 2008, **130**, 13132–13139.

Open Access Article. Published on 11 May 2022. Downloaded on 2/9/2026 7:45:13 AM. This article is licensed under a Creative Commons Attribution-NonCommercial 3.0 Unported Licence.

2 R. E. Blankenship, *Molecular Mechanisms of Photosynthesis*, Blackwell Science Ltd, Malden, USA, 2002.
3 Y. Umena, K. Kawakami, J. R. Shen and N. Kamiya, *Nature*, 2011, **473**, 55–U65.
4 P. Jordan, P. Fromme, H. T. Witt, O. Klukas, W. Saenger and N. Krauss, *Nature*, 2001, **411**, 909–917.
5 M. Medina, *FEBS J.*, 2009, **276**, 3942–3958.
6 J. K. Hurley, G. Tollin, M. Medina and C. Gomez-Morena, in *Photosystem I: the light-driven plastocyanin: ferredoxin oxidoreductase*, Springer, Dordrecht, 2006, pp. 455–476.
7 C. M. Bruns and P. A. Karplus, *J. Mol. Biol.*, 1995, **247**, 125–145.
8 L. Serre, F. M. D. Vellieux, M. Medina, C. Gomez-Morena, J. C. Fontecilla-Camps and M. Frey, *J. Mol. Biol.*, 1996, **263**, 20–39.
9 P. Mulo and M. Medina, *Photosynth. Res.*, 2017, **134**, 265–280.
10 M. E. Corrando, A. Aliverti, G. Zanetti and S. G. Mayhew, *Eur. J. Biochem.*, 1996, **239**, 662–667.
11 M. Faro, C. Gomez-Morena, M. Stankovich and M. Medina, *Eur. J. Biochem.*, 2002, **269**, 2656–2661.
12 M. Martinez-Julvez, J. Hermoso, J. K. Hurley, T. Mayoral, J. Sanz-Aparicio, G. Tollin, C. Gomez-Morena and M. Medina, *Biochemistry*, 1998, **37**, 17680–17691.
13 M. C. Walker, J. J. Pueyo, C. Gomez-Morena and G. Tollin, *Arch. Biochem. Biophys.*, 1990, **281**, 76–83.
14 K. Huang, S.-I. Tu and J. H. Wang, *Biochem. Biophys. Res. Commun.*, 1969, **34**, 48–52.
15 M. Medina, C. Gomez-Morena and R. Cammack, *Eur. J. Biochem.*, 1995, **227**, 529–536.
16 A. Serrano, J. Rivas and M. Losada, *FEBS Lett.*, 1984, **170**, 85–88.
17 J. I. Martinez, P. J. Alonso, C. Gomez-Morena and M. Medina, *Biochemistry*, 1997, **36**, 15526–15537.
18 M. Medina and R. Cammack, *Perkin Trans. 2*, 1996, **2**, 633–638.
19 S. C. Silver, J. Niklas, P. Du, O. G. Poluektov, D. M. Tiede and L. M. Utschig, *J. Am. Chem. Soc.*, 2013, **135**, 13246–13249.
20 S. R. Soltau, P. D. Dahlberg, J. Niklas, O. Poluektov, K. L. Mulfort and L. M. Utschig, *Chem. Sci.*, 2016, **7**, 7068–7078.
21 S. R. Soltau, J. Niklas, P. D. Dahlberg, K. L. Mulfort, O. G. Poluektov and L. M. Utschig, *ACS Energy Lett.*, 2017, **2**, 230–237.
22 S. R. Soltau, J. Niklas, P. D. Dahlberg, O. G. Poluektov, D. M. Tiede, K. L. Mulfort and L. M. Utschig, *Chem. Commun.*, 2015, **51**, 10628–10631.
23 L. M. Utschig, N. M. Dimitrijevic, O. G. Poluektov, S. D. Chemerisov, K. L. Mulfort and D. M. Tiede, *J. Phys. Chem. Lett.*, 2011, **2**, 236–241.
24 L. M. Utschig, S. C. Silver, K. L. Mulfort and D. M. Tiede, *J. Am. Chem. Soc.*, 2011, **133**, 16334–16337.
25 W. Chorney, N. Scully, H. L. Crespi and J. J. Katz, *Biochim. Biophys. Acta*, 1960, **37**, 280–287.
26 H. L. Crespi, S. Archer and J. J. Katz, *Nature*, 1959, **184**, 729–730.
27 H. L. Crespi, S. Conrad, R. A. Uphaus and J. J. Katz, *Ann. N. Y. Acad. Sci.*, 1960, **84**, 648–666.
28 G. Link, T. Berthold, M. Bechtold, J. U. Weidner, E. Ohmes, J. Tang, O. Poluektov, L. Utschig, S. L. Schlesselman, M. C. Thurnauer and G. Kothe, *J. Am. Chem. Soc.*, 2001, **123**, 4211–4222.
29 A. L. Morris, S. W. Snyder, Y. Zhang, J. Tang, M. C. Thurnauer, P. L. Dutton, D. E. Robertson and M. R. Gunner, *J. Phys. Chem.*, 1995, **99**, 3854–3866.
30 J. R. Norris, R. A. Uphaus, H. L. Crespi and J. J. Katz, *Proc. Natl. Acad. Sci. U. S. A.*, 1971, **68**, 625–628.
31 O. G. Poluektov, L. M. Utschig, S. L. Schlesselman, K. V. Lakshmi, G. W. Brudvig, G. Kothe and M. C. Thurnauer, *J. Phys. Chem. B*, 2002, **106**, 8911–8916.
32 R. R. Rustandi, S. W. Snyder, L. L. Feezel, T. J. Michalski, J. R. Norris, M. C. Thurnauer and J. Biggins, *Biochemistry*, 1990, **29**, 8030–8032.
33 J. Tang, L. M. Utschig, O. Poluektov and M. C. Thurnauer, *J. Phys. Chem. B*, 1999, **103**, 5145–5150.
34 M. C. Thurnauer and P. Gast, *Photobiochem. Photobiophys.*, 1985, **9**, 29–38.
35 L. M. Utschig, S. R. Greenfield, J. Tang, P. D. Laible and M. C. Thurnauer, *Biochemistry*, 1997, **36**, 8548–8558.
36 V. Massey, *Biochem. Soc. Trans.*, 2000, **28**, 283–296.
37 H. L. Crespi, J. R. Norris and J. J. Katz, *Biochim. Biophys. Acta*, 1971, **253**, 509–513.
38 C. C. Correll, M. L. Ludwig, C. M. Bruns and P. A. Karplus, *Protein Sci.*, 1993, **2**, 2112–2133.
39 P. W. Riddles, R. L. Blakeley and B. Zerner, *Methods Enzymol.*, 1983, **91**, 49–60.
40 B. Shan, T. Baine, X. A. N. Ma, X. Zhao and R. H. Schmehl, *Inorg. Chem.*, 2013, **52**, 4853–4859.
41 R. Malkin and A. J. Bearden, *Proc. Natl. Acad. Sci. U. S. A.*, 1971, **68**, 16–19.
42 U. Brahmachari, P. R. Pokkuluri, D. M. Tiede, J. Niklas, O. G. Poluektov, K. L. Mulfort and L. M. Utschig, *Photosynth. Res.*, 2020, **143**, 183–192.
43 A. Quaranta, B. Lagoutte, J. Frey and P. Setif, *J. Photochem. Photobiol., B*, 2016, **160**, 347–354.
44 J. J. Pueyo, C. Gomez-Morena and S. G. Mayhew, *Eur. J. Biochem.*, 1991, **202**, 1065–1071.
45 A. Okafuji, A. Schnegg, E. Schleicher, K. Möbius and S. Weber, *J. Phys. Chem. B*, 2008, **112**, 3568–3574.
46 G. Kurisu, M. Kusunoki, E. Katoh, T. Yamazaki, K. Teshima, Y. Onda, Y. Kimata-Ariga and T. Hase, *Nat. Struct. Biol.*, 2001, **8**, 117–121.
47 R. Morales, M. H. Charon, G. Kachalova, L. Serre, M. Medina, C. Gomez-Moreno and M. Frey, *EMBO Rep.*, 2000, **1**, 271–276.
48 G. T. Hanke, G. Kurisu, M. Kusunoki and T. Hase, *Photosynth. Res.*, 2004, **81**, 317–327.
49 P. N. Palma, B. Lagoutte, L. Krippahl, J. J. G. Moura and F. Guerlesquin, *FEBS Lett.*, 2005, **579**, 4585–4590.
50 L. Hammarstrom, *Acc. Chem. Res.*, 2015, **48**, 840–850.
51 A. J. Morris, G. J. Meyer and E. Fujita, *Acc. Chem. Res.*, 2009, **42**, 1983–1993.
52 L. M. Utschig, *Chem*, 2022, **8**, 5–6.
53 O. G. Poluektov and L. M. Utschig, *J. Phys. Chem. B*, 2021, **125**, 4025–4030.

© 2022 The Author(s). Published by the Royal Society of Chemistry

Open Access Article. Published on 11 May 2022. Downloaded on 2/9/2026 7:45:13 AM.
This article is licensed under a Creative Commons Attribution-NonCommercial 3.0 Unported Licence.

54 O. G. Poluektov, L. M. Utschig, A. A. Dubinskij and M. C. Thurnauer, *J. Am. Chem. Soc.*, 2004, **126**, 1644–1645.
55 O. G. Poluektov, L. M. Utschig, A. A. Dubinskij and M. C. Thurnauer, *J. Am. Chem. Soc.*, 2005, **127**, 4049–4059.
56 L. M. Utschig, M. C. Thurnauer, D. M. Tiede and O. G. Poluektov, *Biochemistry*, 2005, **44**, 14131–14142.
57 S. Gould, G. F. Strouse, T. J. Meyer and B. P. Sullivan, *Inorg. Chem.*, 1991, **30**, 2942–2949.
58 L. C. Sun, H. Berglund, R. Davydov, T. Norrby, L. Hammarstrom, P. Korall, A. Borje, C. Philouze, K. Berg, A. Tran, M. Andersson, G. Stenhagen, J. Martensson, M. Almgren, S. Styring and B. Akermark, *J. Am. Chem. Soc.*, 1997, **119**, 6996–7004.
59 H. L. Crespi, U. Smith, L. Gajda, T. Tisue and R. M. Ammeraal, *Biochim. Biophys. Acta*, 1972, **256**, 611–618.
60 K. Tagawa and D. I. Arnon, *Biochim. Biophys. Acta*, 1968, **153**, 602–613.
61 M. M. Bradford, *Anal. Biochem.*, 1976, **72**, 248–254.
62 R. Masaki, K. Wada and H. Matsubara, *J. Biochem.*, 1979, **86**, 951–962.
63 S. Stoll and A. Schweiger, *J. Magn. Reson.*, 2006, **178**, 42–55.